METHODOLOGY FOR THE METHOD OF IMAGES IN TRANSIENT ANALYSIS OF EXTERNAL FAULT ELECTROMAGNETIC FORCES IN POWER TRANSFORMERS

FAUSTO VALENCIA, HUGO ARCOS
Department of Electrical Energy
Escuela Politecnica Nacional, Quito, Ecuador
Email: fausto.valencia@epn.edu.ec
Email: hugo.arcos@epn.edu.ec

Abstract: *In this paper, it is presented a methodology to apply the Method of Images in the determination of transient electromagnetic forces in windings of power transformers due to external faults. Correction factors are introduced in the process of calculus, avoiding the need for iterations. Only four images of the windings and one simulation with both the method of images and the finite element method with the rated current of the transformer are needed for the determination of the correction factors. The method proposed was implemented in C++ and the results were compared to those of the finite element method through simulations performed in the free software Femm 4.2. The simulations exhibit that the correction factors are valid for any value of current circulating through the windings, hence, they can be used for transient analysis of the forces, where the current is variable. The method of images, as described here, perform transient analysis in much less time than the finite element method.*

Key words: *Computational electromagnetics, electromagnetic forces, electromagnetic transients, finite element analysis, power transformers.*

1 Introduction

During the process of design, power transformers are verified that they can withstand the electromagnetic forces presented when there are high currents in the system, mainly in the case of external short circuit events [1]. These forces are usually calculated from a static point of view, by considering a constant current circulating through the windings, whose value is generally that of the steady state of the fault, as it has been done in [2].

On the other hand, sometimes it is necessary to know the behaviour of the equipment under transient conditions; for example, when analysing internal vibrations of the windings and of the core [3]. This brings out a problem since the response of the conductor material of the windings is different when operating under transient conditions [4].

Both, static and transient phenomena are commonly analysed with the finite element method (FEM), mainly when the displacement current can be neglected, like in low - frequency signals. There is no problem for the study of the static case; however, the transient event requires a FEM simulation of each step of time, as it is shown in [5]. Besides, each simulation involves several iterations to assure the convergence of the method, a subject that by itself is a topic under analysis [6].

One of the alternatives for the transient analysis of forces is the Method of Images (MOI). Minhas in his dissertation [7] used this method for the determination of electromagnetic forces in Power Transformers. Four images were located on the sides of the core, and four images were added for each iteration. In this model, the disks were reduced to conductive filaments which caused the existence of a small error when compared with FEM. The results were used in a dynamic model to investigate the effects of vibrations in the behaviour of the pressboard, and were tested in a physical model so that it was clearly validated.

On the other hand, Masood Moghaddami [8], used the MOI for the determination of electromagnetic forces in the busbars that connect the low voltage winding of an arc furnace transformer with its terminals. Masood shows an analytical development to calculate the forces between the bars. Moreover, the images employed were not limited to the four sides of the core, but there were also images in the four corners; this increased the number of images to eight on the first iteration, twelve on the second iteration and so on. With those modifications, the results of MOI were very close to the results of FEM, giving good convergence so that the tolerance was reached on the second iteration. However, the analytical approach is not possible in the analysis of the forces in the winding because the disks are not parallel as the bars, except for those located at the same *x* or *y* coordinate, such

Table 1. Characteristics of the Windings

Item	Low Voltage Winding	High Voltage Winding
Number of Disks	60	68
Width of Disk [cm]	3.96	5.4
Height of Disk [cm]	1.15	0.98
Insulation of Disk [cm]	0.4	0.4
Turns per disk	4	18
Internal radius [cm]	17.65	24.01
Winding resistance [Ω]	0.2842	4.43
Winding inductance [mH]	8.272	128
Rated current [A]	262.43	51.4

Table 2. Characteristics of the Core

Item	Value
Diameter of the Leg [cm]	32.8
Window Height [cm]	104.04
Window Width [cm]	30.71

Fig. 1. Equivalent circuit for the transformer for the simulation of a fault at its terminal.

as the disks of the same winding.

In that regards, the main idea of this paper is to show a new way to analyse transient electromagnetic forces in reduced time, by using MOI without iterations and applying only four images and correction factors that could be determined with basic data of the transformer. To show the process, a one phase transformer was modelled with MOI and FEM; the results are compared and statistically analysed to find their range of difference.

2   Case Study

The transformer under study is a one phase adaptation of the three-phase 33/11 kV, $\Delta - Y$ 5 MVA two winding transformer designed in [9]. Table 1 shows the geometrical dimensions of its windings and Table 2 shows the dimensions of the core. Given by the design in percentage, the series resistance is 0.678 % and the leakage reactance is 7.44 %.

For the current, we considered a transient due to a fault at the terminals of the low voltage side of the transformer. Thus, the transformer could be modelled as an R-L series circuit (see Fig. 1), whose current was calculated by (1). The angle ψ defines the power factor of the transformer, as shown in (2) and θ is an angle introduced to control the instant of closing the circuit. V_m is the maximum voltage coming from the source and ω is its angular frequency which, for a 60 Hz system, has a value of 377 rad/s (For an exhaustive derivation of the expression see [4]).

$$i = \frac{V_m}{\sqrt{(R^2 + \omega^2 L^2)}} \left[\sin(\omega t + \theta - \psi) - \sin(\theta - \psi)\exp(-\frac{R}{L}t) \right] \tag{1}$$
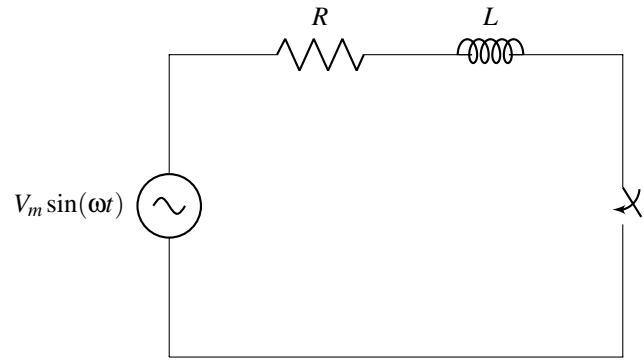
$$\cos\psi = \frac{R}{\sqrt{(R^2 + \omega^2 L^2)}} \tag{2}$$

Represented in the low voltage side of the transformer ($Z_{BASE} = 24.2\Omega$), the combined resistance for both windings is 0.1641 Ω, whereas the leakage reactance is 1.8 Ω, i.e. an inductance of 4.775 mH.

The data of the system and transformer are replaced in (1) to determine the current in the low voltage winding i_{LV}. The angle θ is set to zero so that a fault at time zero is analysed. In the expression, the peak voltage phase to neutral was used.

$$i_{LV} = \frac{11 \cdot 10^3 \sqrt{2}/\sqrt{3}}{\sqrt{0.1641^2 + 377^2(4.775 \cdot 10^{-3})^2}}$$
$$\left[\sin(377t - 1.47988) + \sin(1.47988)e^{-34.366t} \right]$$

Hence, the current used in the simulations for the low voltage winding is

$$i_{LV} = 4969[\sin(377t - 1.47988) - \sin(-1.47988)\exp(-34.36t)]A \tag{3}$$

Whereas for the high voltage side the current obtained was

$$i_{HV} = 974.31[\sin(377t - 1.47988) - \sin(-1.47988)\exp(-34.36t)]A \tag{4}$$

The fault current for the low voltage side of the transformer is shown in Fig. 2.

3   Method of Images for Power Transformers

Under an external fault, the core of the transformer has high permeability, i.e. it is a good conductor of magnetic field (see Fig. 3). Hence, we could create an image of the
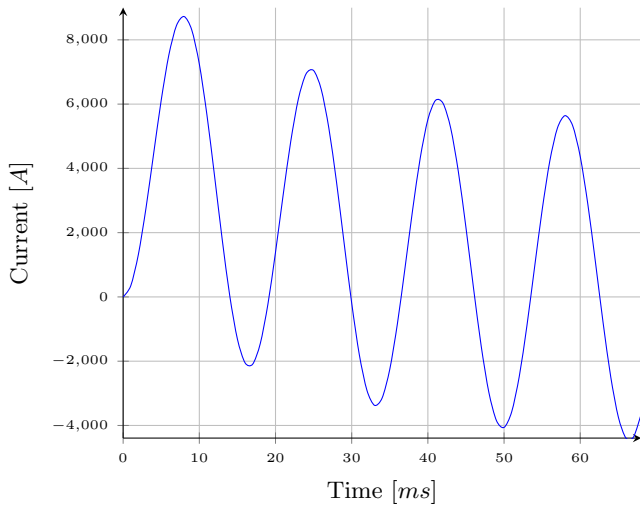
Fig. 2. Current through the low voltage winding during a short circuit fault.
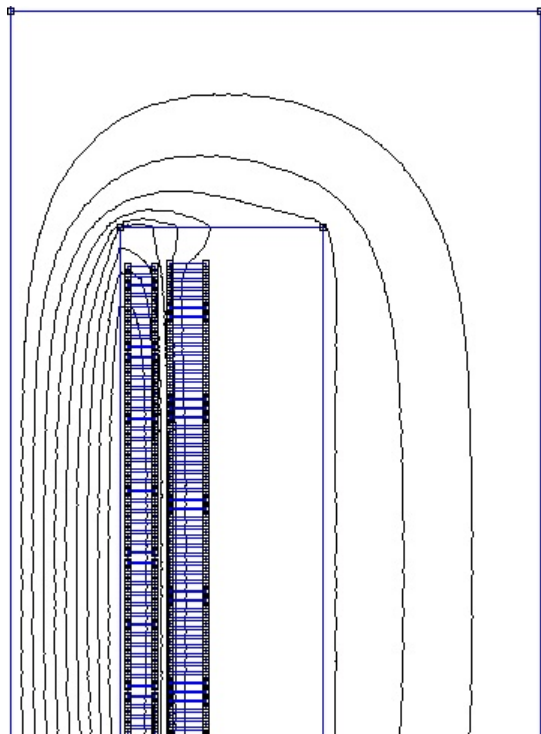

Fig. 4. Images of the windings in four sides of the core.

Fig. 3. Equipotential lines of the magnetic field in the core of a power transformer.

Fig. 5. Conductive filaments replace the rectangular disks inside the core window.

1. The disks that are rectangles in their original form are reduced to conductive filaments. As a consequence, the geometry of the disks is not considered (See Fig. 5).
2. The saturation of the core is neglected because we analysed only short circuit currents which bring low voltages so that the core does not work overexcited. For this reason, the value of the current in the images is the same as that of the windings.
3. The filaments that represent the disks have a straight path, along the z axis in the two dimensional representation. The length of these conductors is the mean circular perimeter of the low and high voltage windings.

winding with the same current, without losing too much precision. The line dividing the insulating material and the core works as the mirror.

Fig. 4 shows the images created on the four sides of the mirror, and the direction of the current circulating through the windings. MOI is applied in two dimensions, thus the currents are directed in the z axis and the magnetic field is located in the x, y plane. The currents symbolized as points mean they are in the positive z axis, whereas those represented by an x mean they are in the negative z axis.

Some assumptions have been made in modelling the transformer with MOI:
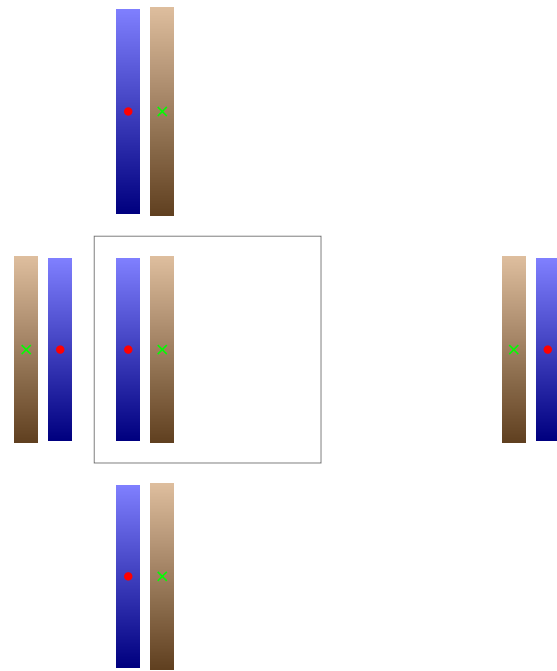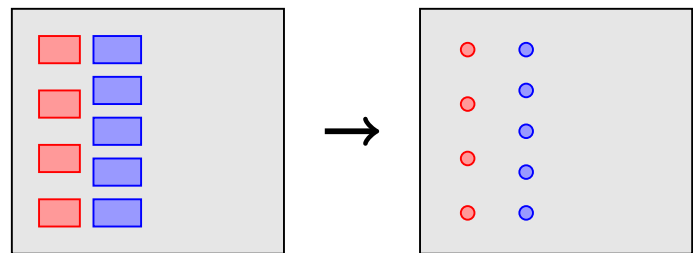
3.1 Electromagnetic force calculation

Once the images are created, the forces can be calculated by (5) which represents the force between two parallel conductors of length L, with a current I_1 and I_2, and a relative position vector **r**. This equation is applied to every pair of conductors involved in the calculation, i.e. the conductors of the windings and those of the images.

$$\mathbf{F} = -\frac{\mu_0 I_1 I_2}{2\pi r^2} L\mathbf{r} \qquad (5)$$

The total force is calculated for each conductor as the sum of the forces of each pair. The pairs of conductors must consider every winding. For example, for the first disk (the highest one) of the low voltage conductor, the pair of conductors must be formed with the rest of the disks of the low voltage windings, all disks of the high voltage windings, and all disks of the four images of both windings.

In its normal procedure, MOI must be applied iteratively. Additional images are created on each iteration until the desired tolerance is achieved in the value of the force [10]. We have found in this investigation that neither the additional images nor iterations are needed when using the correction factors.

An object-oriented program was developed in C++ for the implementation of MOI as described here. No iterations were included in the algorithm since only one image per side is used in the process.

3.2 Correction factors

This investigation proposes the use of correction factors applied to the module of the forces resultant from one simulation of MOI. Those factors represent the relation between the module of the force coming from MOI and that of FEM.

Fig. 6 shows the relative difference between the simulation results of FEM and MOI that were performed with the current calculated with (3) and (4). Note that the relative differences do not depend on the time, i.e. they do not depend on the value of the current through the windings. According to this outcome, we could take a ratio between the values resultant from both methods and make it valid for the whole transient phenomenon.

In Fig. 7 the procedure to determine the correction factors is shown. With the geometry of the transformer and the rated current, simultaneous simulations are performed with FEM and MOI. Finally, for each disk, the correction factors are found by the division between the forces obtained with MOI and those obtained with FEM. This procedure must be performed once in a transformer lifetime, the correction factors can be used for any value of current and, therefore, for any transient phenomenon.

Table 3 and Table 4 show the correction factors for some disks of the low voltage and high voltage windings.

Once the correction factors are obtained, they must be applied to every transient analysis performed with MOI. Fig. 8 shows the procedure to apply the correction factors to any transient analysis of electromagnetic forces where MOI has been employed. Notice that the factors are applied to the module of the force.
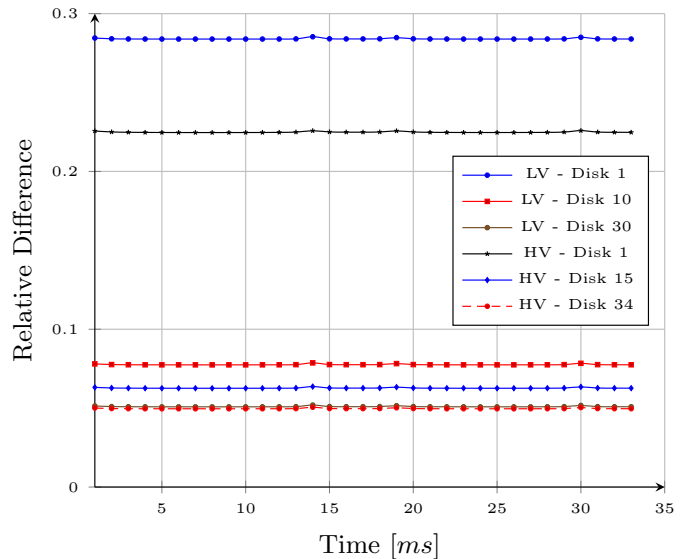

Fig. 6. Relative differences between the results of FEM and MOI along time.

Table 3. Results for FEM and MOI simulations of the Low Voltage Winding and Correction Factors - Disks 1, 11 and 30.

Disk	FEM Force (N)	MOI Force (N)	Correction Factor
1	57.11	73.35	1.2844
11	63.54	68.50	1.0780
30	64.76	68.08	1.0513

Table 4. Results for FEM and MOI simulations of the High Voltage Winding and Correction Factors - Disks 1, 15 and 34.

Disk	FEM Force (N)	MOI Force (N)	Correction Factor
1	40.25	49.30	1.2248
15	55.78	59.30	1.063
34	57.29	60.16	1.05

4 Modelling the transformer for Finite Element Analysis

The FEM simulations were performed with the software *Femm 4.2*, which basically allows the analysis of electro and magnetostatic two-dimensional problems. The program has been widely used for the analysis of magnetic fields in windings of power transformers like in [11].

External faults are power frequency phenomena, therefore the displacement current could be neglected and (6) can be used for this problem.

$$\nabla^2 \mathbf{A} = \mathbf{J} \qquad (6)$$

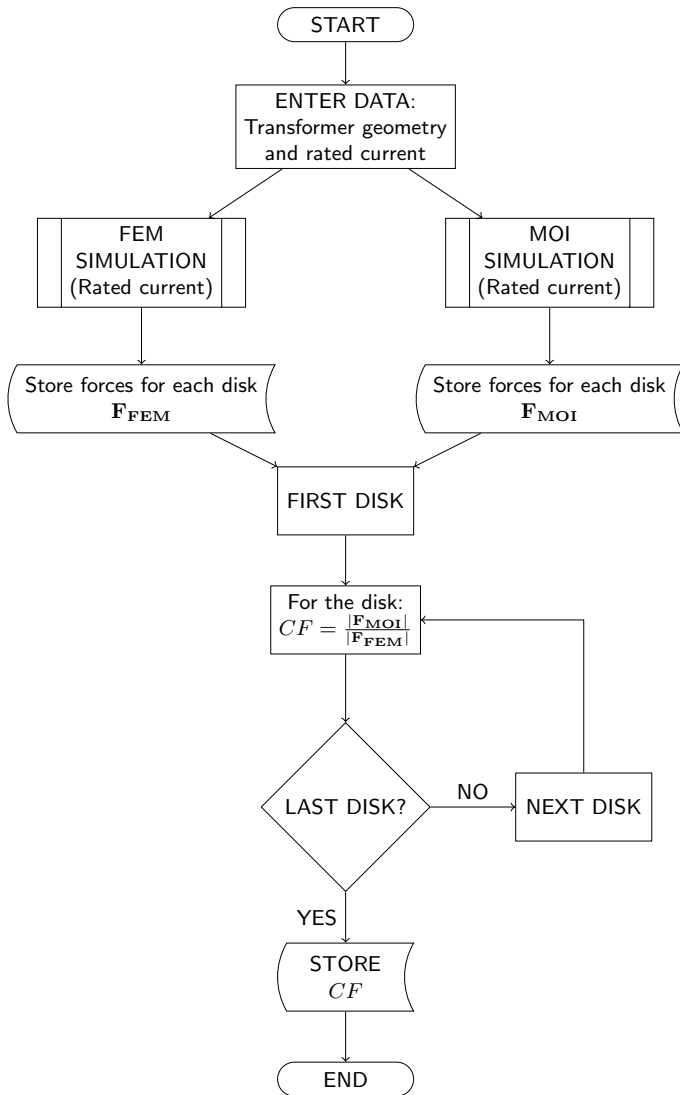The initial data for the problem is shown in Fig. 9. The

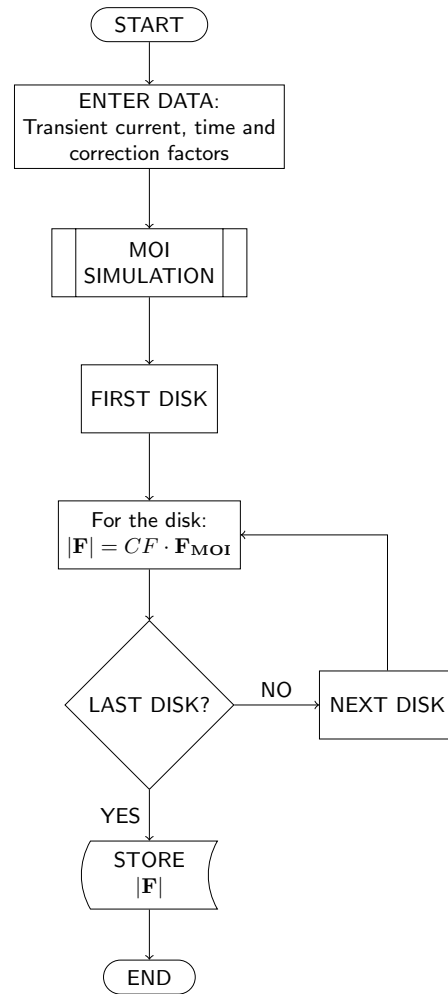Fig. 7.   Flowchart for the determination of the correction factors (CF).

Fig. 8.   Flowchart for the utilization of the correction factors in a transient analysis of electromagnetic forces.

depth is used for the program to consider a volume where the forces are going to be determined, in this case, its value is the same as the length of the conductive filaments described in Section 3. The *Problem Type* has two options: planar or axial; the option *axial* would create a cylindrical transformer, which is not the case under study, therefore we chose the option *planar*. The rest of the data is used by *Femm 4.2* for the iterations during the simulation.

Fig. 10 shows the implementation of the transformer in *Femm 4.2*. In Fig. 10a, there is a semicircle that represents the contour where the border conditions have been applied; for the analysis of the transformer, the vector magnetic potential $\mathbf{A}$ has been set to zero, i.e. we have implemented a condition of Dirichlet in the border.

In the model implemented in *Femm 4.2*, the plane is divided into regions that represent the material of the physical model. This material can be chosen from the options given by the software. For the model of the transformer, we chose the following material:
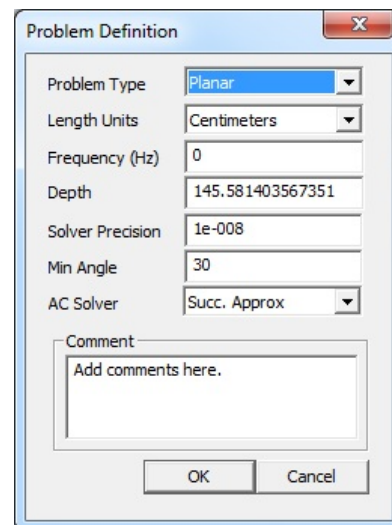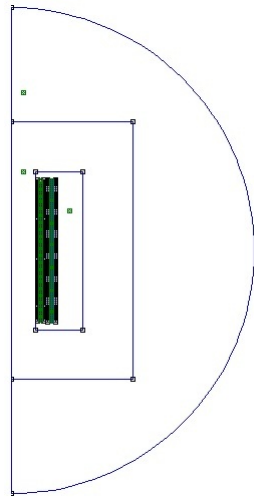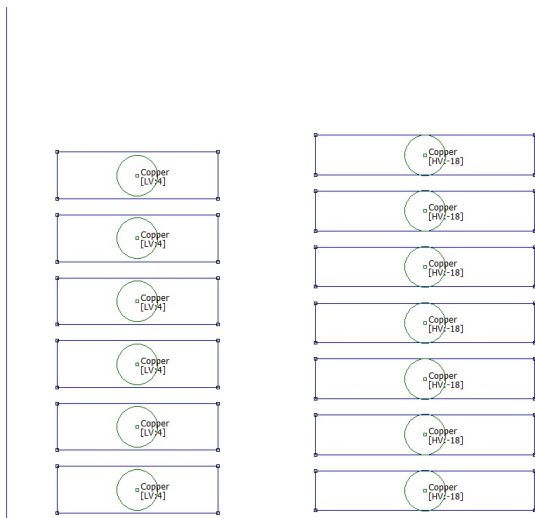

Fig. 9.   Initial data for the implementation of the transformer in Femm 4.2.

The region that surrounds the core is filled with *Air*. The region between the windings and the core is *Air*. *US Steel Type 2-S 0.018 inch thickness* was used for the

(a) Complete view, including the border.

(b) Detailed upper disks of the two windings.

Fig. 10. FEM implementation of the transformer in the software Femm 4.2.

core.

The material for the windings is *Copper*

In Fig. 10b the disks of the windings are detailed and they are modelled in *Femm 4.2* by a circuit with four turns for the low voltage winding and 18 turns for the high voltage winding. The direction of the current is represented by its sign on each disk. Half of the transformer geometry was entered in the program in order to reduce the time of simulation.

Once the transformer data was entered into *Femm 4.2*, we made use of the library *Pyfem* of Python which can vary the input data of the program and can control the execution of the case. Thus, we entered the current as a function of time, and for each millisecond, one simulation was run and the results were saved for one pre-established disk. These steps were repeated for 33 *ms*.
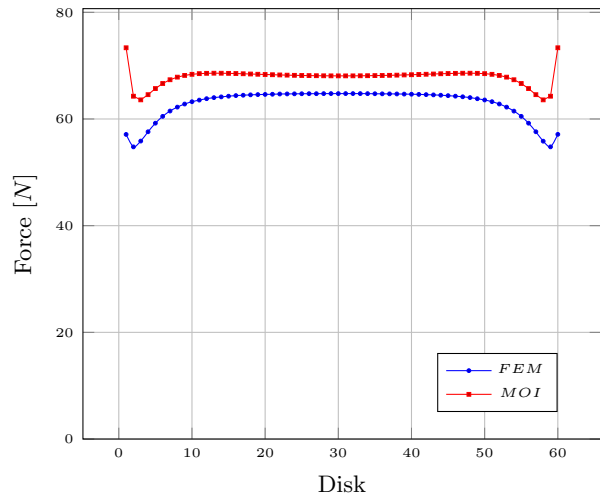

Fig. 11. Forces obtained with FEM and MOI, on the disks of the low voltage winding.
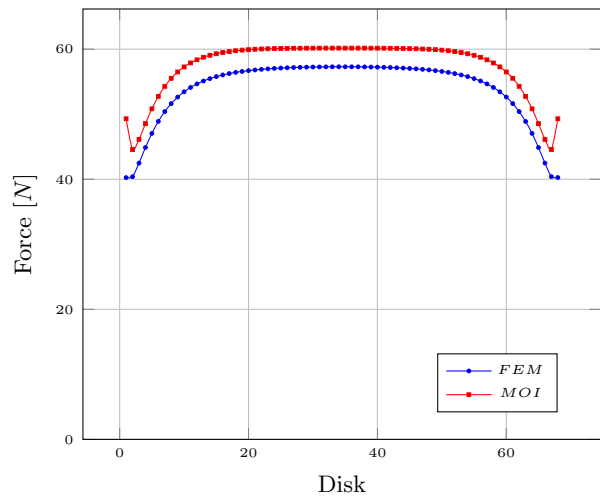

Fig. 12. Forces obtained with FEM and MOI, on the disks of the high voltage winding.

5 Results

5.1 Static Case

Fig. 11 and Fig. 12 show the module of the forces obtained by using FEM and MOI in all disks, 60 disks for the low voltage winding and 68 disks for the high voltage winding. The simulations were performed with the rated currents, and the results were used for the determination of the correction factors. The results for MOI are always higher than those of the FEM simulation, the behaviour of the forces is similar along the winding, and the highest differences are in the top disks.
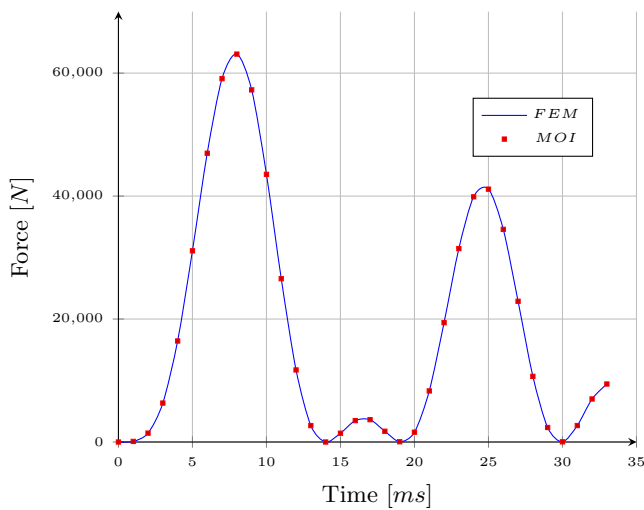
5.2 Transient simulation

Fig. 13 and Fig. 14 show the results of the simulation for the first 33 *ms* of the fault current with and without the correction factor. Notice that after the correction factors are applied, there is no difference between the results.

For a time of 33 *ms*, Table 5 shows the mean value of
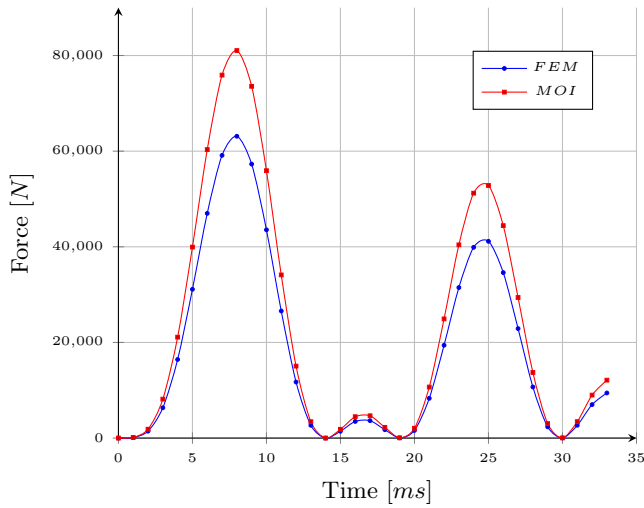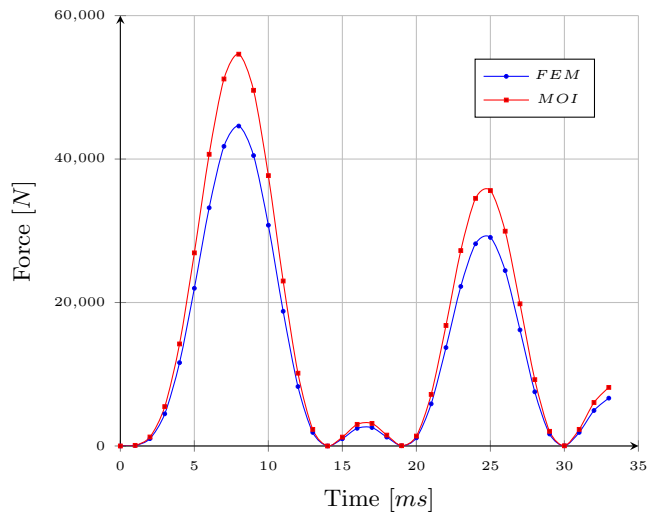
(a) without the correction factor
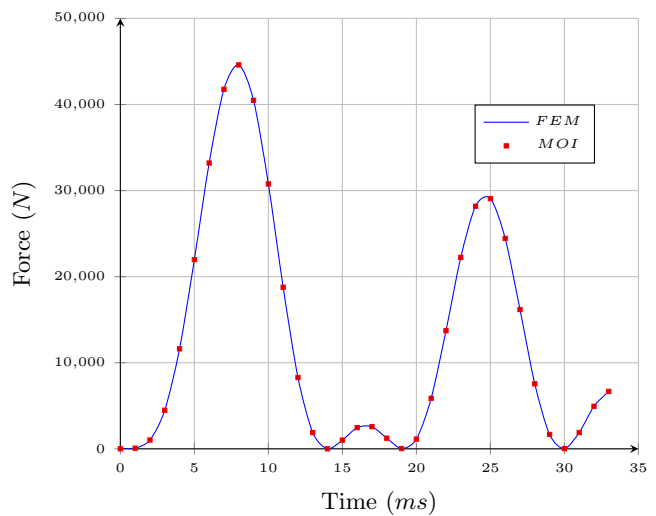

(b) with the correction factor

Fig. 13. Force on Disk 1 of the low voltage winding with FEM and MOI.

(a) without the correction factor

(b) with the correction factor

Fig. 14. Force on Disk 1 of the high voltage winding with FEM and MOI.

the relative difference in percentage, the standard deviation and the range of relative difference, considering a level of confidence $\alpha = 0.01$ in a t-student statistical analysis.

Table 6 shows the time spent in the simulation with FEM and with MOI without iterations. It is clearly noted that the method proposed in this research reduces the time of simulation in more than one hundred in a case with 34 steps.

6 Conclusion

In this research, it has been shown that the Method of Images can be used in the transient analysis of the electromagnetic forces that affect the windings during short circuit events. This is achieved with the use of correction factors that equate the results of FEM and of the Method of Images. As a consequence, the same results are obtained in much less time. The implementation of the proposed method is simpler than similar approaches due to the elimination of iterations during the process.

In future investigations, the method could be extended to the analysis of different types of transformers, inrush phenomenon, switching events, etc. In this sense, the understanding of the behaviour of the equipment inside the power system could be enhanced.

Table 5. Statistical behaviour of the differences between FEM and MOI under a level of confidence of 0.01.

Disk	Mean value	Range of Difference [%]
LV - 1	0.026325819	0.01370 to 0.03895
LV - 11	0.03601911	0.02288 to 0.04916
LV - 30	0.029360039	0.01746 to 0.04126
HV - 1	-0.007770035	-0.02062 to 0.005078
HV - 15	0.022366549	0.01097 to 0.03376
HV - 34	0.024990109	0.01461 to 0.03537

Table 6. Time for simulations with FEM and MOI.

Disk	FEM [s]	MOI [s]
LV - 1	2 990	22.19
LV - 11	3 044	22.17
LV - 30	3 091	23.33
HV - 1	2 913	22.19
HV - 15	2 953	22.73
HV - 34	3 079	22.47

References

1. H. M. Ahn, J. Y. Lee, et.al., "Finite-element analysis of short-circuit electromagnetic force in power transformer," *IEEE Transactions on Industry Applications*, Vol. 47, No. 3, 1267–1272, 2011.

2. C. M. Arturi, "Electromagnetic force calculations on a 3-phase autotransformer under time-varying fault by a 3D non-linear finite element code,"*IEEE transactions on magnetics* , Vol. 29, No. 2, 2010–2013, 1993.

3. S. Saponara, L. Fanucci, "Predictive diagnosis of high-power transformer faults by networking vibration measuring nodes with integrated signal processing" *IEEE Transactions on Instrumentation and Measurement*, Vol. 65, No. 8, 1749–1760, 2016.

4. A. Greenwood, "Simple Switching Transients" in *Electrical transients in power systems* , John Wiley and Sons Inc., New York, 1991.

5. H. Zhang, B. Yang, W. Xu, et.al., "Dynamic deformation analysis of power transformer windings in short-circuit fault by FEM", *IEEE Transactions on Applied Superconductivity*, Vol. 24, No. 3, 1–4, 2014.

6. K. Hoffman, et.al., "A Vector Jiles–Atherton Model for Improving the FEM Convergence", *IEEE Transactions on Magnetics* , Vol. 53, No. 6, 1–4, 2017.

7. M. Minhas, "Dynamic behaviour of transformer winding under short-circuits", PhD thesis, University of the Witwatersrand, Johannesburg, 2008.

8. M. Moghaddami, A. Moghadasi, "An algorithm for fast calculation of short circuit forces in high current busbars of electric arc furnace transformers based on method of images",*Electric Power Systems Research*, Vol. 136, 173–180, 2016.

9. I. Dasgupta,"Design of the 5 MVA, 33/11 kV Transformer", in *Design of transformers*, McGraw-Hill Education, New Delhi, 2002.

10. S. Kulkarni, S. Khaparde, "Impedance Characteristics", in *Transformer Engineering, Design and Practice*, CRC Press, 2004.

11. R. Pile, et.al. "Comparison of main magnetic force computation methods for noise and vibration assessment in electrical machines", *IEEE Transactions on Magnetics* Vol. 54, No. 7, 1–13, 2018.